UC San Diego

Title

Different Oxidative Stresses Lead to Phenotypic Heterogeneity of Homogenous Yeast Cells

Permalink

https://escholarship.org/uc/item/9wd6586q

Author

Wang, Yifei

Publication Date

2021

UNIVERSITY OF CALIFORNIA SAN DIEGO

Different Oxidative Stresses Lead to Phenotypic Heterogeneity of Homogenous Yeast Cells

A thesis submitted in partial satisfaction of the requirements

for the Master of Science degree

in

Biology

By

Yifei Wang

Committee in charge:

Professor Nan Hao, Chair
Professor Lorraine Pillus, Co-Chair
Professor Katherine Petrie

2021

The Thesis of Yifei Wang is approved, and it is acceptable in quality and form for publication on microfilm and electronically.

University of California San Diego

2021

TABLE OF CONTENTS

LIST OF FIGURES

ACKNOWLEDGEMENTS

I would like to thank Professor Nan Hao for providing the opportunity and wonderfully collaborative lab environment to complete this study, and Professor Lorraine Pillus for providing advice for my research.

I would also like to thank the members of the Hao Lab for their collaboration and guidance especially Dr. Yanfei Jiang, Dr. Zhen Zhou, and Yu-Chieh Lee.

ABSTRACT OF THE THESIS

Different Oxidative Stresses Lead to Phenotypic Heterogeneity of Homogenous Yeast Cells

By

Yifei Wang

Master of Science in Biology

University of California San Diego, 2021

Professor Nan Hao, Chair

Professor Lorraine Pillus, Co-Chair

The phenotypic heterogeneity in isogenic cells draws the attention of researchers since it is considered a main strategy of cells to adapt to various stresses in the environment. It is strongly related to the cellular redox status because the differences in the regulation of redox status are a known cause of this heterogeneity and because oxidative stresses are a major type of environmental threats. Previous studies have applied hydrogen peroxide to yeast cells to

demonstrate the homeostatic plasticity in H_2O_2 stress response. In this study, a series of innovative methods were integrated to unravel the characteristics and mechanism of the phenotypic heterogeneity in homogenous yeast cells under 3 kinds of oxidative stresses. The main technique used was the combination of microfluidic platform and time-lapse microscopy, which enabled us to record the fluorescence of single yeast cells in the environment with or without oxidative stresses. The fluorescence data generated went through the process of segmentation and classification using MATLAB and Python transcripts. The application of K-Means clustering algorithm provided more insights into the distinct types of stress responses. Consequently, not only did we identify the distinct phenotypes of GFP fluorescence change in single yeast cells under different types of oxidative stresses, but we also made and tested some hypotheses on the stress response mechanisms. Among the statements we made in the study, the most crucial one should be that the ability to regulate intracellular pH played an important role in the heterogeneity of stress responses. The intriguing patterns in the K-Means results were also explored with a large number of related questions to be answered in future research.

INTRODUCTION

       Phenotypic heterogeneity refers to the phenotypic differences between genetically identical cells grown in homogenous environments [1]. It increased the population fitness by increasing the diversity of cells to cope with fluctuating environments [1]. One major domain of heterogeneity is the cellular redox status, since it affects numerous cellular functions including proliferation, protein homeostasis, and aging [2]. On one hand, individual differences in redox status can give rise to distinct subpopulations among isogenic cells; on the other hand, oxidative stresses are a major type of environmental stresses to which the cells try to adapt [2]. Specifically, stress tolerance is an exemplary case of cellular adaptation in which a mild stress preconditioning increases the resistance of cells so that they would be less affected by subsequent exposure to large doses of the same stressor [3]. Previous studies have used the response of yeast *S. cerevisiae* to stresses like hydrogen peroxide (H_2O_2) as a model to investigate the driving principles of protein homeostasis and cellular aging. This model is popular because yeast cells divide asymmetrically, which means cellular components are partitioned unequally between the mother and daughter cells. The mother cell keeps more volume and thus more damage factors related to aging in cell division [4]. While the daughter cells can have full replicative potential, we could also measure the number of cell divisions of a mother cell before its death, also defined as the replicative lifespan (RLS) [5].

       Protein homeostasis, or proteostasis, refers to a network that acts to maintain proteins in the appropriate concentration, conformation, and subcellular location to help achieve cellular stability. The accuracy of this system is considered essential to ensure robust physiological adaptation [3]. In Goulev's study, they performed a comprehensive analysis of the characteristics of yeast cell responses under H_2O_2 stress in which they controlled the concentrations of H_2O_2 to

quantitatively analyze the mechanism of adaptative homeostasis [3]. They proposed that the adaptation of cells to the stress is dependent on the response time of the cellular homeostatic machinery [3]. In their experiment settings, they also found a RLS extension after preconditioning with very low doses of H_2O_2 [3]. Therefore, this system is naturally connected to the aging of yeast cells.

Cellular aging is a complex and dynamic process driven by various types of stresses that lead to cellular damage [4]. In previous research, we found that yeast cells can age through two distinct pathways caused by either DNA unsilencing or mitochondrial damage [4, 6, 7]. The major promoting factor in yeast cell aging is the advances in microfluidic technology, which enables us to measure the fluorescence of individual cell continuously during its aging process [4]. By combining the microfluidic platform with time-lapse microscopy and computational modeling, we could apply different types of oxidative stresses to yeast cells with certain amount, measure their adaptive stress response accurately, and then analyze the heterogeneous aging dynamics in yeast cells [4].

Following a similar track, this research focuses on the phenotypic heterogeneity of genetically homogeneous yeast cells under different types of oxidative stresses. The hypothesis is that the cell-to-cell variability in oxidative status results in distinct stress responses and aging types under different oxidative stresses. In our research, microfluidic experiments were conducted using yeast strains tagged with fluorescent proteins including the green fluorescent protein (GFP), mCherry (a member of monomeric red fluorescent proteins), and the near-infrared fluorescent protein (iRFP). Throughout the research, three kinds of common oxidizing agents were applied as the oxidative stress: hydrogen peroxide (H_2O_2), diamide, and KCl. The synthetic defined medium (abbreviated as SD medium hereafter) was used as the solvent for all four

stressors. The behaviors of yeast cells under these stresses, as well as the change in aging phenotype and population, were studied to construct a model to explain the mechanism of phenotypic heterogeneity.

METHODS

2.1 Yeast strain construction

Standard methods for the growth, maintenance, and transformation of yeast strains and for manipulation of DNA were used throughout the research. The three yeast strains used in this study were generated from the BY4741 (MAT a his3Δ1 leu2Δ0 met15Δ0 ura3Δ0) strain background and their detailed information was listed below:

NH874: BY4741, NHP6a-iRFP:Kan; pTDH3::pTDH3-mCh-URA3;

NH1284: BY4741, NHP6a-iRFP:Kan; pTDH3-pRS306-pGPD-GFP; DCP2-mCherry-LEU;

NH1435: BY4741, NHP6a-iRFP:Kan; pTDH3-sfpHluorin-CYC1 terminator-URA; DCP2-mCherry-LEU.

To make the nuclear-anchored iRFP reporter, an iRFP fragment was amplified and integrated into the C-terminus of NHP6a at the native locus by homologous recombination. Similarly, a mCherry-URA3 or mCherry-LEU fragment was amplified and integrated into the C-terminus of pTDH3 or DCP2 genes by homologous recombination. The pTDH3-pGPD-GFP reporter was made by ligation into the pRS306 vector. Furthermore, MRV55, a superfolder pHluorin for improved intracellular pH measurements, was tagged on pTDH3 using a similar approach. This pH sensor is more sensitive than normal GFP and is modified to perform ratiometric imaging to extract absolute pH values [8].

All transformations were performed with the standard lithium acetate method, and integration was confirmed by PCR.

2.2 Microfluidic device and time-lapse microscopy

The microfluidics experiments were performed as described in the introduction part and in Hansen's article [9]. Yeast cells were inoculated into 2 ml of SD medium and cultured overnight. 2 ml of saturated culture was diluted into 20 ml of SD medium and grown overnight until it reached $OD600_{nm}$ of ~0.4. For loading, cells were diluted in ~3 ml and transferred into the microfluidic device, a multi-channel solenoid made of PDMS [9]. To keep cells immobile in the microfluidic device during time-lapse experiments, we added concanavalin A, a lectin that binds cell surface saccharides, to the microfluidic device [9]. The device was connected to plastic tubing (TYGON, ID 0.020 IN, OD 0.060 IN, wall 0.020 IN) and the other side was put into either SD medium or the solution containing stressors. They were pumped into the device by adjusting the relative height difference between the input medium flask and waste flask [9].

Time-lapse microscopy was performed using a Nikon Ti-E inverted fluorescence microscope with Perfect Focus, coupled with an EMCCD camera (Andor iXon X3 DU897). The light source is a Spectra X LED system. Images were taken using a CFI Plan Apochromat Lambda DM X60 oil immersion objective (NA 1.40 WD 0.13MM). The microscope was programmed to acquire images for each fluorescence channel every 2 min. Each experiment last for 6 hours and 10 minutes, with the first 10 minutes as the baseline (only SD medium flowed through cells). Then 2 h of oxidative stress was applied, during which only the solution containing oxidizing agents flowed through cells. In the last cycle of the stress period, the

entrance of stress solution was blocked, and SD medium flowed through cells again for 4 h as the recovery time.

A simplified version of microfluidics experiments, the slides capture, was also performed with similar settings. The yeast cells were inoculated and diluted in the same approach. When the $OD600_{nm}$ of cells were in the appropriate range, a small volume of the cells (~10 uL) were applied to a slide and their fluorescence was captured by the microscope. Then the oxidative stress reagents were added into the flasks containing cells for 2 hours of the stress time. Another photo of fluorescence would be taken at the end of the 2-hour period. A pH meter was used to measure the pH of the solution before adding the oxidizing reagents and after 2 hours of stress.

2.3 Image analysis and quantification

Four types of fluorescence were used in the experiments: phase to observe the physical conditions of cells, green fluorescence to detect GFP signal, mCherry fluorescence to detect mCherry signal, and the near-infrared fluorescence to detect iRFP signal. Fluorescence images were processed with a custom MATLAB code as described in Hansen's article [9]. The cytoplasm and the nucleus of single cells were identified by thresholding the iRFP nuclear marker and the phase image. The time series data of fluorescence intensity was segmented by a custom MATLAB code and then clustered by K-Means algorithm using Jupiter Notebook. In the process of clustering, the elbow method was used to find the appropriate number of centers (k in the K-Means algorithm). The Elbow method consists of plotting the variation as a function of the number of clusters and picking the elbow of the curve as the number of clusters to use.

RESULTS

3.1 Identification of the distinct responses of cells to H_2O_2 stress

The initial discovery of the phenomenon that homogenous yeast cells responded differently to H_2O_2 stress on a single-cell level was made in a microfluidics experiment using yeast strain NH1284 when we found that there were several patterns of GFP intensity change within a group of cells. To demonstrate this phenomenon clearly, we did another microfluidics experiment using 4 concentrations of H_2O_2 stress: 0.25 mM, 0.5 mM, 0.75 mM, and 1 mM. Two snapshots from the time series are presented as an instance of the different patterns of GFP intensity changes (Figure 1). The time point of these snapshots was at the 124th frame (186 frames in total); in other words, in the total 6 hours of experiment, the snapshots show the conditions at 4 h. We could observe that in the middle of the recovery period, some cells have demonstrated restored GFP fluorescence while others remained dark.

After acquiring the time series data, we used a custom MATLAB code to segment the fluorescence. This code assigned a small area as one cell based on the nuclear marker with iRFP fluorescence and then calculated the average intensity of GFP or mCherry fluorescence of this area. The outputs of this code are spreadsheets which could be processed to identify the responses of each cell to H_2O_2 stress using clustering methods in Python. Before clustering, we wanted to know how many clusters we should divide the data into, so we performed the Elbow method and demonstrated the result of optimal number of clusters for the data of NH1284 under all concentrations of H_2O_2 stress (Figure 2). Since we needed to pick the "elbow" of the curve that fits the entire range of concentrations, we chose k=3 as the number of clusters for most of the heatmaps plotted below. The only exception happened when we analyzed the data of NH1284 cells under KCl stress and will be explained in detail later.
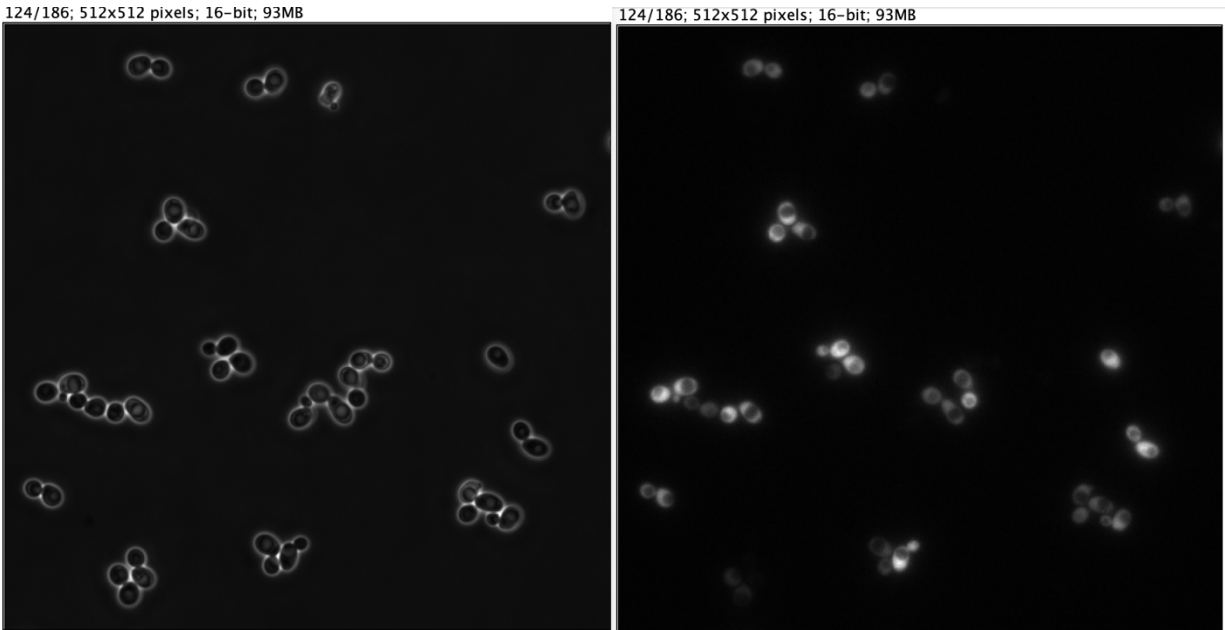
Figure 1. The snapshots of the time series data on strain NH1284 cells. The timepoint of these snapshots were at frame 124/186 (2/3 of the total time). The left image was taken under the phase light and the right image was taken under GFP fluorescence.
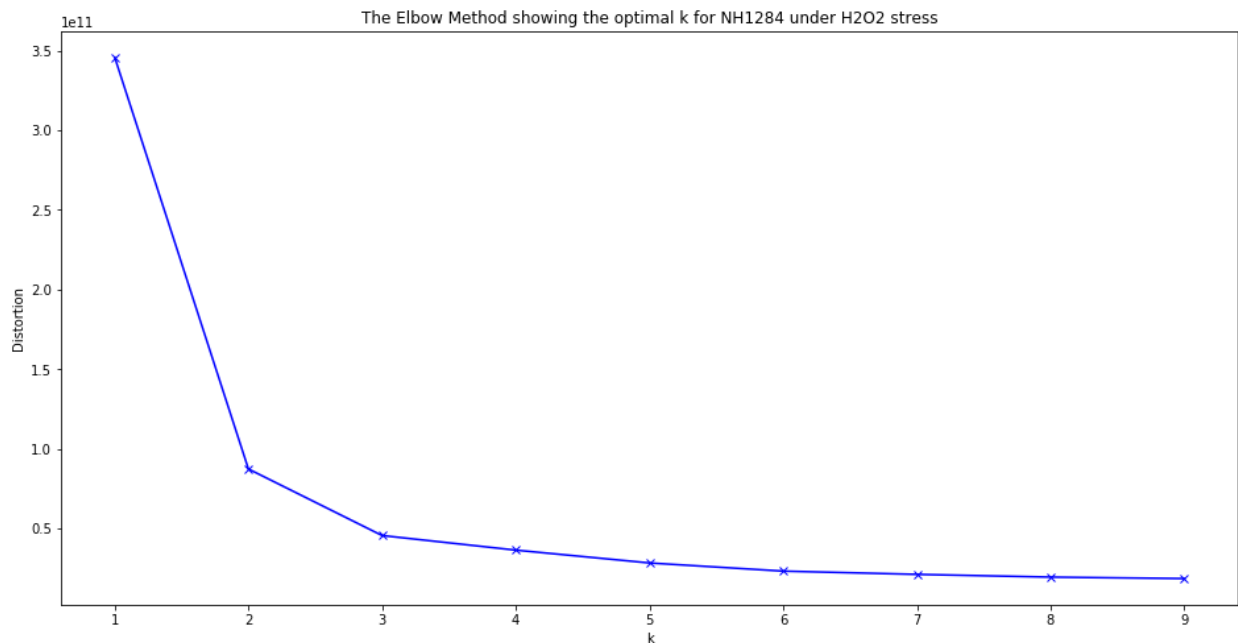
Figure 2. The plot of the elbow method used on the data of NH1284 cells under H_2O_2 stress. The x-axis lists the first 9 numbers of k which represents the number of clusters used in the classification. The y-axis shows the distortion score, in other words, the sum of square distances from each point to its assigned center.

Since we had determined to use k=3 as the number of clusters, we continued the analysis by using K-Means algorithm to cluster the data of treating NH1284 strain with 4 concentrations of H_2O_2 stress. We combined the data of average GFP intensity from 4 concentrations into a total set, labelled each cell with cluster 1/2/3 based on the results of K-Means algorithm, and plotted the GFP intensity traces of each cell in heatmaps (Figure 3). In these heatmaps, each horizontal line represents one cell segmented based on the iRFP nuclear marker. Its GFP intensity trace from frame 1 to frame 186 is demonstrated by the brightness of the color; the brighter the color is, the higher the GFP intensity is. At frame 62, the 2-hour-moment when the H_2O_2 stress was

removed, a blue vertical line is drawn on the heatmap to indicate the switch of stages of the experiment.

From these 4 heatmaps we could see that there are 3 types of traces. Type 1 is the cells that never had their GFP intensity dropped to the level around 2000. When 0.25 mM H_2O_2 stress was applied, almost all cells belonged to this category (Figure 3A). A few cells from 0.5 mM H_2O_2 stress were also Type 1 (Figure 3B). Type 2 cells were the most intriguing kind, because their GFP intensity dropped below 4000 after H_2O_2 stress was applied but recovered after the stress was removed. Although the time for each Type 2 cell to recover was different, they certainly raised their GFP intensity to the level around 8000 at the end of the experiment. This type of cells mainly showed in 0.5 mM H_2O_2 stress trial and consisted of a small group of cells in 0.75 mM H_2O_2 stress trial (Figure 3BC). The rest of cells from 0.5 mM, 0.75 mM and almost all cells from 1 mM H_2O_2 stress comprised Type 3 cells, of which the GFP intensity dropped to the level around 2000 and never rose until the end of the experiment (Figure 3BCD). From these observations, we could ensure that there were 3 kinds of distinct responses of yeast cells to different concentrations of H_2O_2 stress.
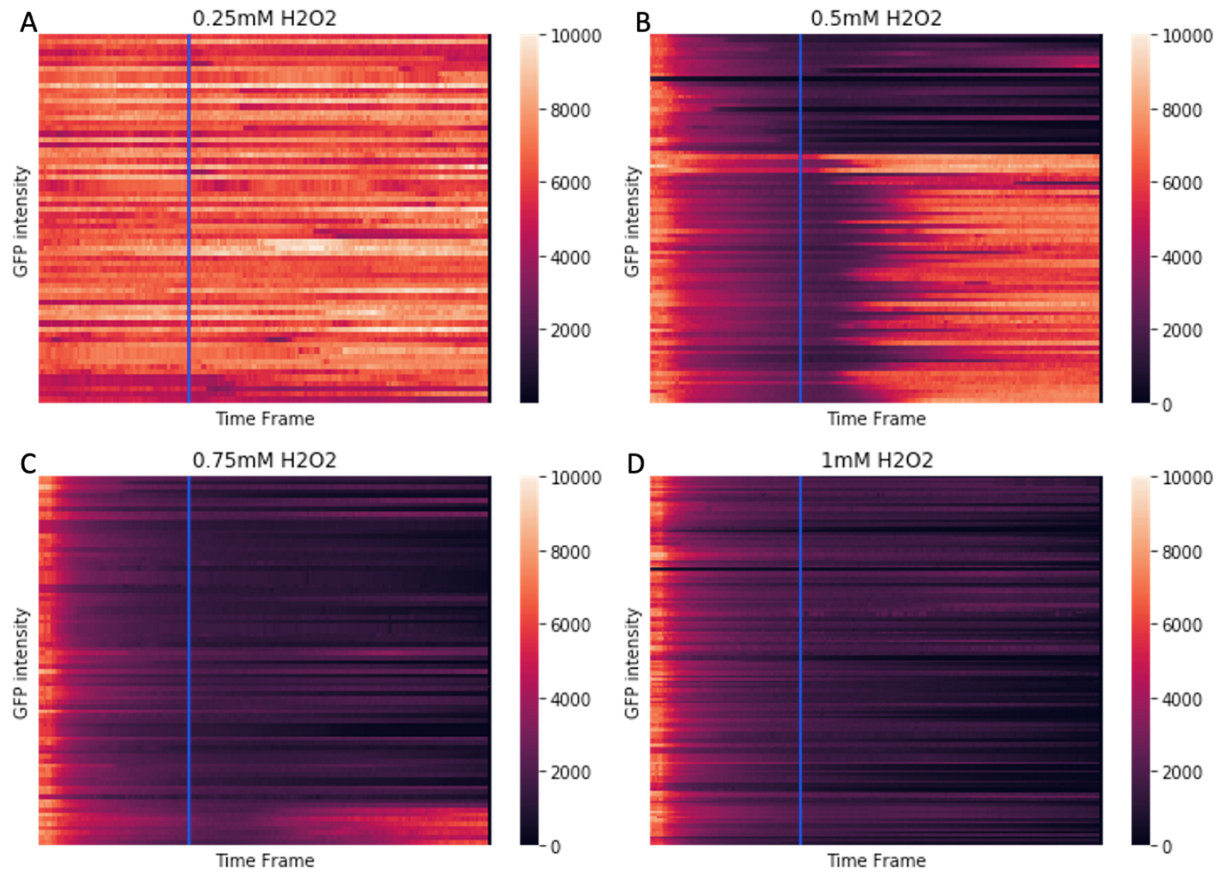
Figure 3. Heatmaps of clustering results of NH1284 cells under 4 concentrations of H_2O_2. In all panels, the x-axis stands for the time frame of the experiment from 1 to 186; the y-axis represents the intensity of GFP fluorescence within a range of 0 to 10000. The blue line in the plots is the x=62 line, which corresponded to the moment when the stress-containing solution stopped entering the cells. (A) Heatmap of the clustering result of NH1284 cells under 0.25 mM of H_2O_2 solution. (B) Heatmap of the clustering result of NH1284 cells under 0.5 mM of H_2O_2 solution. (C) Heatmap of the clustering result of NH1284 cells under 0.75 mM of H_2O_2 solution. (D) Heatmap of the clustering result of NH1284 cells under 1 mM of H_2O_2 solution.

- 10 -

3.2 Exploration of the mechanism for the distinct stress responses

The confirmation of the distinct stress responses of yeast cells to H_2O_2 stress intrigued us to explore the mechanism behind the phenomenon. Since H_2O_2 is a common reactive oxygen species that changes the cellular pH during its oxidizing reaction, our primary hypothesis states that the distinct stress responses resulted from the difference in the cells' ability to regulate their intracellular pH under oxidizing environment. To test this hypothesis, we constructed the yeast strain NH1435 which contains the superfolder pHluorin. Then we repeated the experiment using 4 concentrations of H_2O_2 stress on NH1435 cells (Figure 4). It is evident that the responses of cells could also be categorized into 3 types. Type 1 cells, the ones that remained a high intensity of GFP, appeared mainly in 0.25 mM H_2O_2 (Figure 4A); Type 2 cells, which showed significant recovery of GFP intensity after dropping, were a major part of cells in 0.5 mM H_2O_2 (Figure 4B); the cells in 0.75 mM and 1 mM H_2O_2 mostly consisted of Type 3 cells that could not recover after their GFP intensity dropped to a low level (Figure 4CD). The major difference between Figure 3 and 4 was the distribution of 3 types of cells in 0.5 mM H_2O_2. In Figure 3B, Type 3 cells consisted of 1/3 of cells, while they only consisted of 1/8 of cells in Figure 4B. In contrast, the proportion of Type 2 cells increased significantly in Figure 4B.
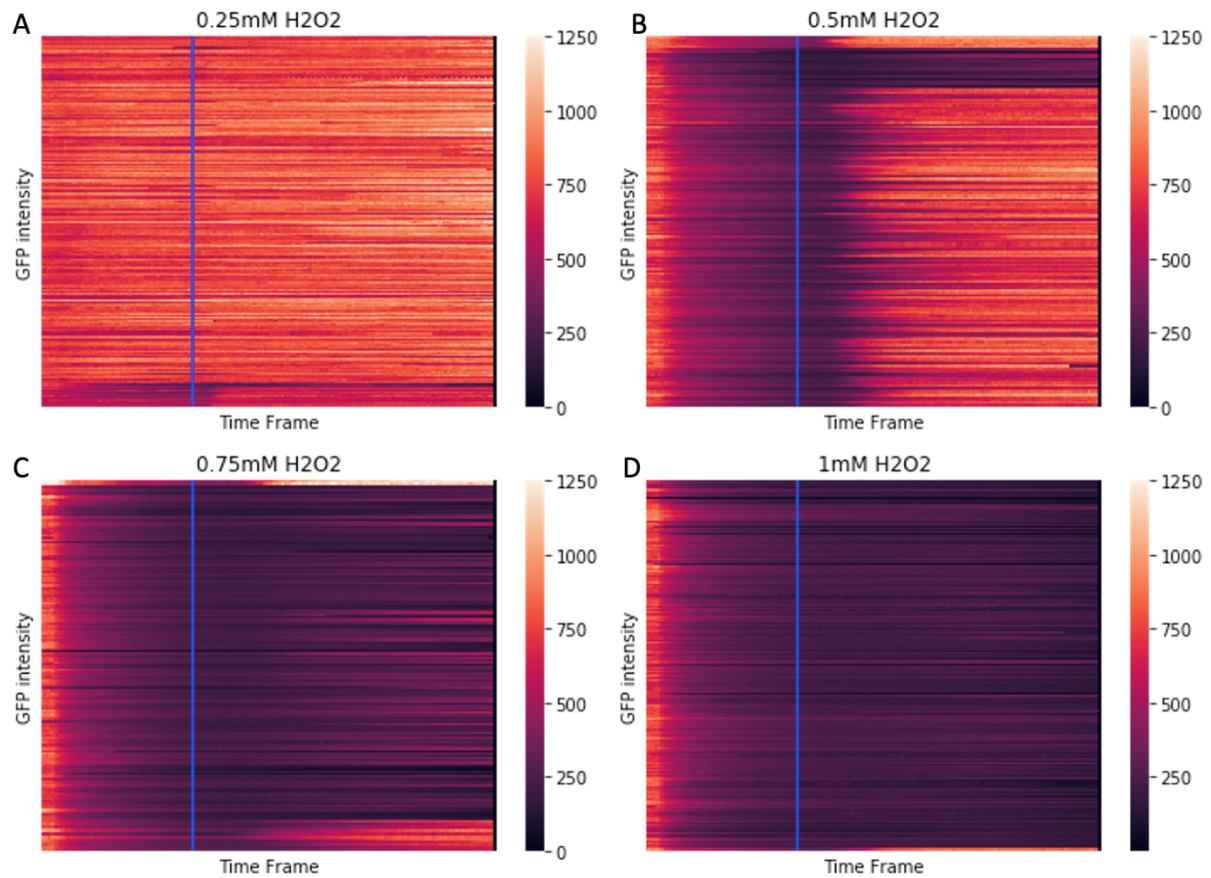
Figure 4. Heatmaps of clustering results of NH1435 cells under 4 concentrations of H_2O_2. In all panels, the x-axis stands for the time frame of the experiment from 1 to 186; the y-axis represents the intensity of GFP fluorescence within a range of 0 to 1250. The blue line in the plots is the x=62 line, which corresponded to the moment when the stress solution stopped entering the cells. (A) Heatmap of the clustering result of NH1435 cells under 0.25 mM of H_2O_2 solution. (B) Heatmap of the clustering result of NH1435 cells under 0.5 mM of H_2O_2 solution. (C) Heatmap of the clustering result of NH1435 cells under 0.75 mM of H_2O_2 solution. (D) Heatmap of the clustering result of NH1435 cells under 1 mM of H_2O_2 solution.

Additionally, it was necessary to eliminate the possibility that the vector pTDH3 we used in the construction of our strains was subject to the oxidative stresses. As a result, we constructed the strain NH874 with mCherry tagged on this vector and performed the same experiment using H_2O_2 stress (Figure 5). As the heatmap shows, under all concentrations of H_2O_2, the intensity of mCherry remained high and there were no patterns of distinct stress responses shown in all cells. We thus proved that the distinct stress responses were only demonstrated by GFP fluorescence in yeast cells.
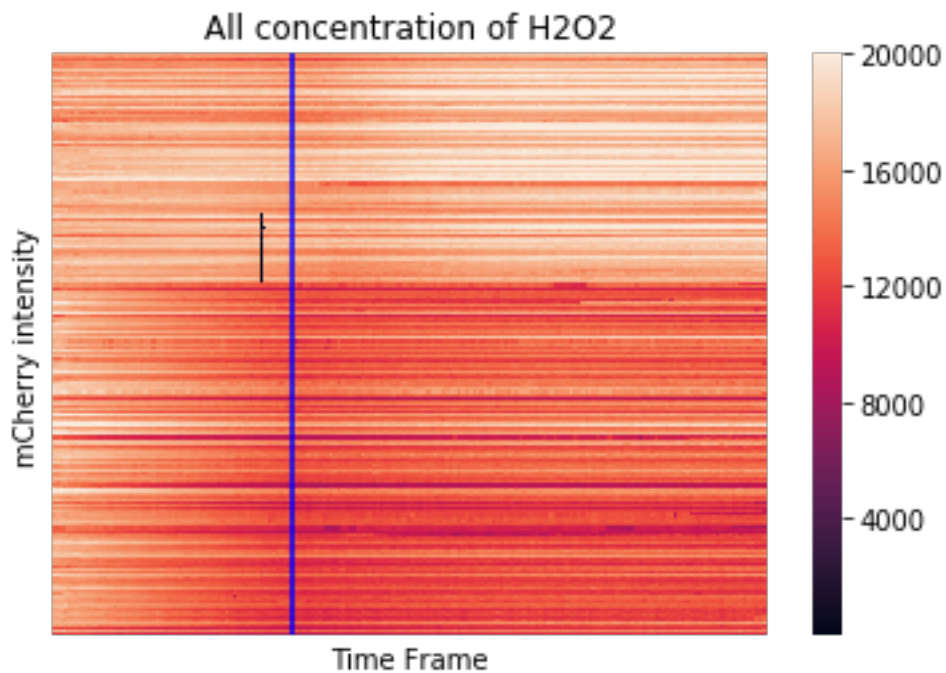

Figure 5. Heatmap of clustering result of NH874 cells under 4 concentrations of H_2O_2. The x-axis stands for the time frame of the experiment from 1 to 186; the y-axis represents the intensity of mCherry fluorescence within a range of 0 to 20000. The blue line in the plots is the x=62 line, which corresponded to the moment when the stress solution stopped entering the cells.

In the process to connect the distinct stress responses with intracellular pH changes, we noticed that we were not able to track the real-time pH of the solution in the chip in the microfluidics experiments. So we designed a simplified version of microfluidics experiment, in which we used slides to take a photo of the fluorescence of cells instead of time series. In this way, we could measure the pH of the solution before we added H_2O_2 to the final concentration of 0.5 mM and measure again after 2 hours of the stress time. To show the distribution of the probability density of the data, we made violin plots (Figure 6). This kind of plots clearly demonstrate that pHluorin had a higher sensitivity to the change of pH in the environment. The distribution of GFP intensity at two levels of pH was similar in NH1284 cells (Figure 6A) but significantly different in NH1435 cells (Figure 6B).

From these two sets of comparison between Figure 3 and Figure 4, Figure 6A and 6B, we consider it testified that the regulation of intracellular pH was strongly related to the change of the GFP intensity in cells. Specifically, we assumed that 0.5 mM H_2O_2 stress was an "appropriate" concentration that was effective in decreasing the pH of the solution but not extremely acidic to suppress the cells' regulation of their intracellular pH to recover the GFP intensity. In such condition, most of NH1435 cells with pHluorin tended to recover their GFP signal as long as they successfully increased their pH level after the stress was removed, whereas a large amount of NH1284 cells kept the GFP intensity low. Although we were unable to unravel the entire mechanism of the distinct oxidative stress responses from yeast cells, we recognized the regulation of intracellular pH as a major factor in the mechanism.
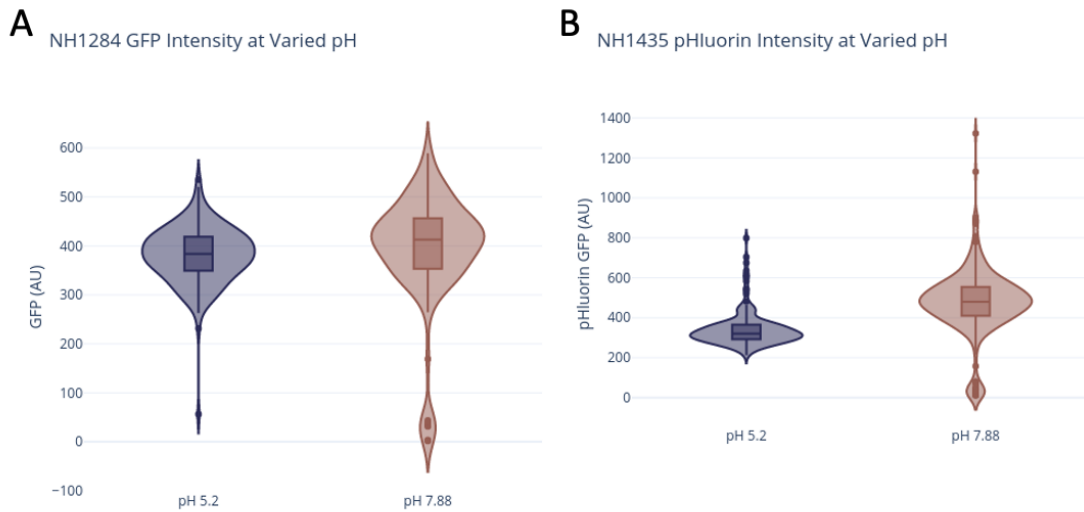
Figure 6. The distribution of GFP/pHluorin intensity at different pH. In both panels, the y-axis represents the intensity of GFP or pHluorin. Two different pH conditions are indicated on the x-axis. The "pH 7.88" condition represents that the photo was taken before H_2O_2 was added to the solution with cells; the "pH 5.2" condition represents that the photo was taken after 2 hours of incubating the cells with 0.5 mM H_2O_2. (A) The violin plot showing the distribution of GFP intensity of NH1284 cells at two pH conditions. (B) The violin plot showing the distribution of pHluorin intensity of NH1435 cells at two pH conditions.

3.3 Seek of other reagents for oxidative stresses

      In addition to the main mechanism, the responses to other type of oxidative stresses were also interesting. Diamide, a common thiol oxidizing agent, was first selected. We applied 4 concentrations of diamide to NH1284 cells and acquired some unexpected results (Figure 7). The primary difference was the characteristics of Type 2 and 3 cells. Although Type 1 cells remained a high level of GFP intensity in the entire experiment, Type 2 cells seemed to stay at a low level of GFP intensity the whole time. There seemed to be no recovery when diamide was used; instead, in Type 3 cells, the GFP intensity decreased to an even lower level after the stress was removed. As for the distribution of each type, most cells still belonged to Type 1 cells in the lowest 4 mM diamide concentration; in 5 mM condition, all three types of cells emerged; in 6 mM and 7 mM conditions, most cells stayed at a low level of GFP as Type 2 cells (Figure 7). The proportion of Type 3 cells were approximately 1/3 in 5 mM, 6 mM, and 7 mM conditions.

      To validate the diversity of characteristics of cells under different stressors, we tested another oxidizing agent, KCl. Following the same process, we applied four concentrations of KCl to NH1284 cells. This time, the intriguing phenomenon started from the Elbow method part (Figure 8). The curve became so smooth from k=2 that we had to select 2 as the number of clusters in further analysis.
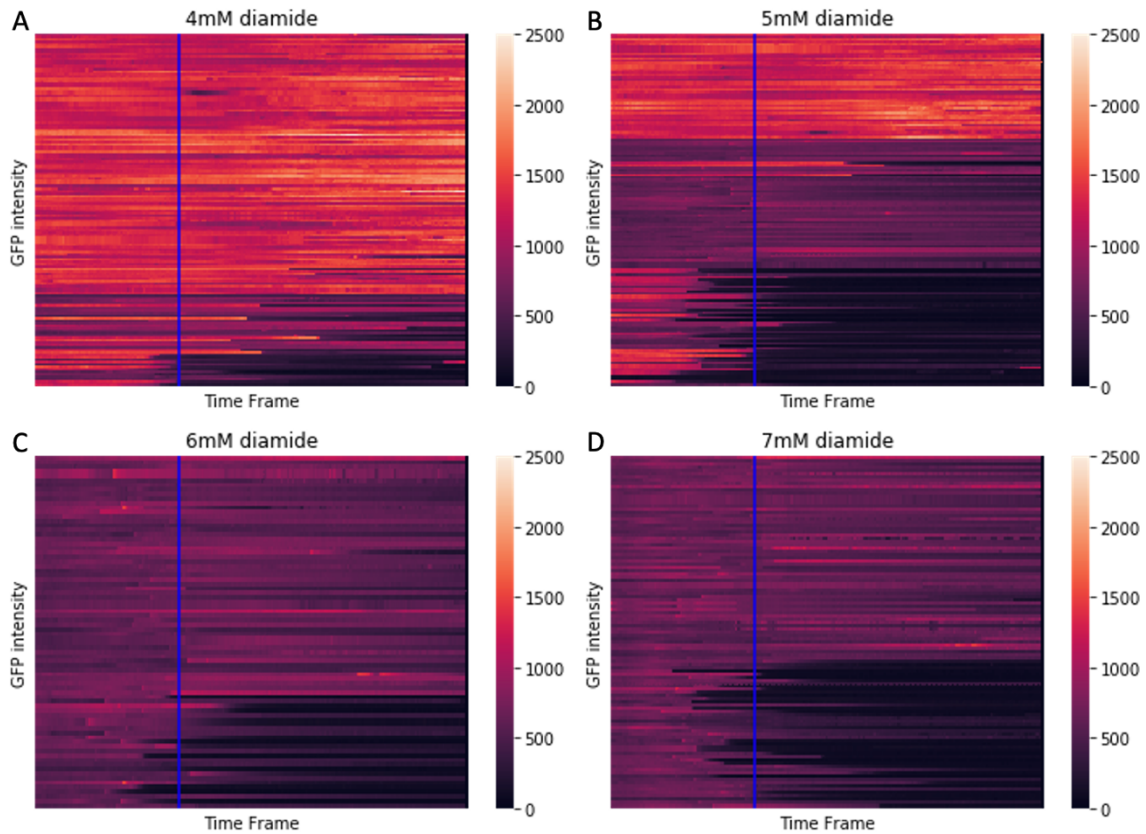
Figure 7. Heatmaps of clustering results of NH1284 cells under 4 concentrations of diamide. In all panels, the x-axis stands for the time frame of the experiment from 1 to 186; the y-axis represents the intensity of GFP fluorescence within a range of 0 to 2500. The blue line in the plots is the x=62 line, which corresponded to the moment when the stress solution stopped entering the cells. (A) Heatmap of the clustering result of NH1284 cells under 4 mM of diamide solution. (B) Heatmap of the clustering result of NH1284 cells under 5 mM of diamide solution. (C) Heatmap of the clustering result of NH1284 cells under 6 mM of diamide solution. (D) Heatmap of the clustering result of NH1284 cells under 7 mM of diamide solution.
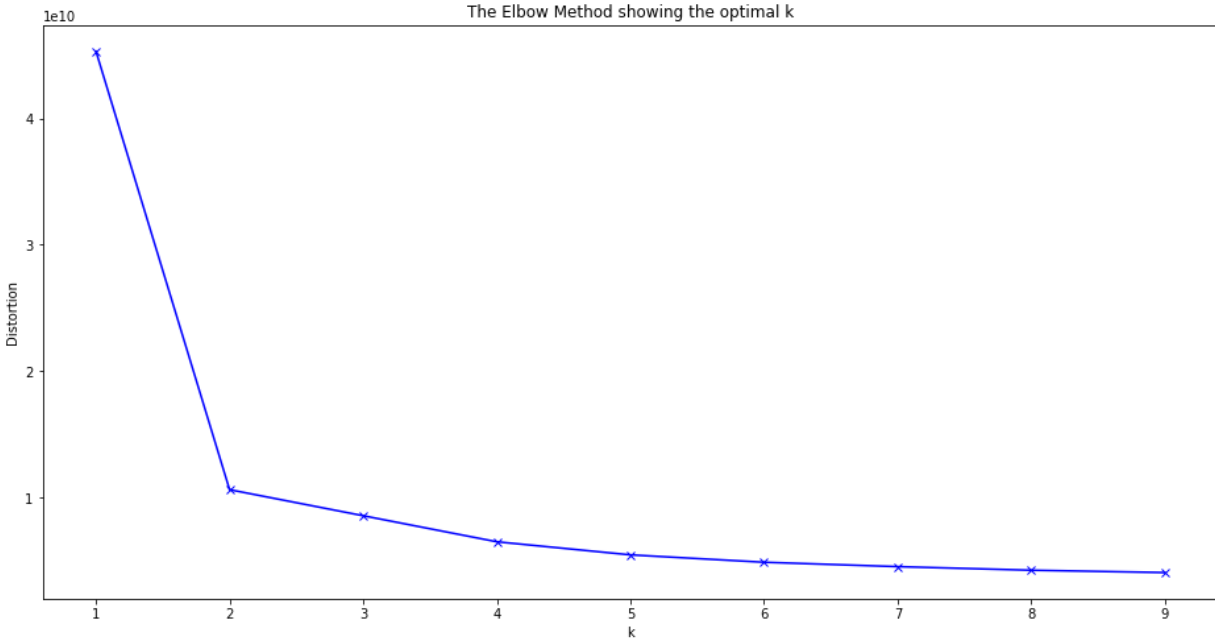
Figure 8. The plot of the elbow method used on the data of NH1284 cells under KCl stress. The x-axis lists the first 9 numbers of k which represents the number of clusters used in the classification. The y-axis shows the distortion score, in other words, the sum of square distances from each point to its assigned center.

Indeed, as the heatmaps revealed, there were only two types of cell stress responses in this experiment (Figure 9). It became more interesting as both types of cells had a high level of GFP during the stress period. In fact, if we take a closer look at the first several frames when KCl solution had not been added, the GFP intensity were even lower (Figure 9). Quickly after the stress was removed, the GFP intensity of two types of cells diverged. Type 1 cells had their GFP intensity dropped to a similar level to that before KCl was added; in type 2 cells, the GFP intensity dropped drastically to a very low level with no sign of recovery thereafter (Figure 9).
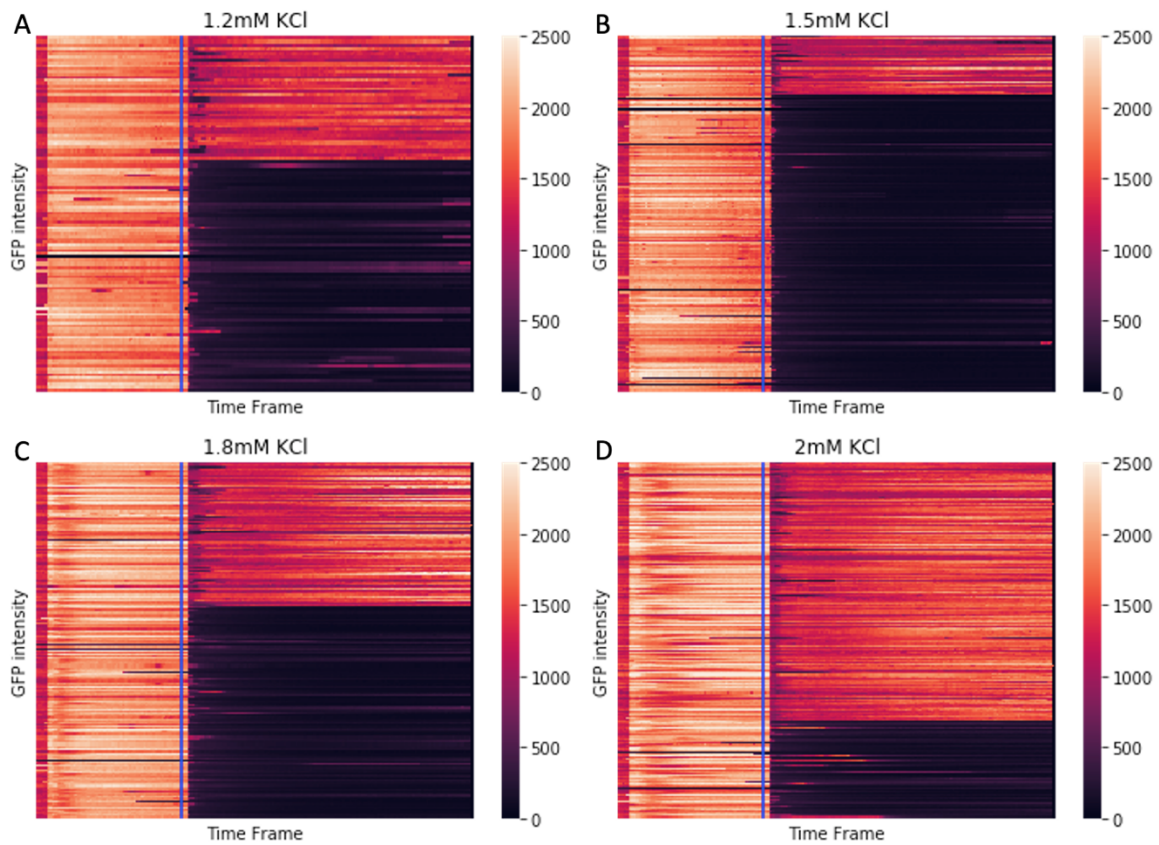
Figure 9. Heatmaps of clustering results of NH1284 cells under 4 concentrations of KCl. In all panels, the x-axis stands for the time frame of the experiment from 1 to 186; the y-axis represents the intensity of GFP fluorescence within a range of 0 to 2500. The blue line in the plots is the x=62 line, which corresponded to the moment when the stress-containing solution stopped entering the cells. (A) Heatmap of the clustering result of NH1284 cells under 1.2 mM of KCl solution. (B) Heatmap of the clustering result of NH1284 cells under 1.5 mM of KCl solution. (C) Heatmap of the clustering result of NH1284 cells under 1.8 mM of KCl solution. (D) Heatmap of the clustering result of NH1284 cells under 2 mM of KCl solution.

With these plots, we could summarize the characteristics of yeast cells' responses to these 3 types of oxidative stresses by generating Figure 10 with the heatmaps of all cells in each of the experiment. When H_2O_2 was used as the stress, the cells varied in their ability to regulate their intracellular pH. Under low concentrations of H2O2, most cells were able to adapt to the change of pH and thus remained a high level of GFP intensity or recovered from the decrease. As the concentration of H2O2 increased, more and more cells failed to regulate their intracellular pH and could not recover from the stress (Figure 3, 4, 10AB).

Situations became different in the diamide experiment. We proposed that besides the change of pH, diamide brought another kind of damage on cells which received two responses: the cells were either not affected by it from the beginning or they bore the pressure the whole time. Also, this damage might suppress the pH changing effect. Consequently, the cells with both pH regulatory ability and resistance to such damage had a high level of GFP intensity the whole time; the cells that carried one of the two abilities stayed at a similar level of GFP intensity after diamide was removed; the rest of cells that were not able to adapt to the change of pH and were affected by such damage had their GFP intensity dropped to an even lower level after the stress was removed (Figure 7, 10C).

The case of KCl stress was more surprising in that almost all cells had a relatively higher GFP intensity during the stress period (Figure 9,10D). Nearly half of cells could return to the similar level of GFP intensity as soon as KCl solution was removed but the other half could not. A possible explanation was that KCl increased the pH of the solution a bit even it is an oxidizing agent. However, the damage from the oxidative stress, like the circumstance in diamide stress, still existed. Therefore, the resistant cells went back to the normal level of GFP intensity, and the affected cells fell to a low level of GFP intensity immediately after the stress was removed.
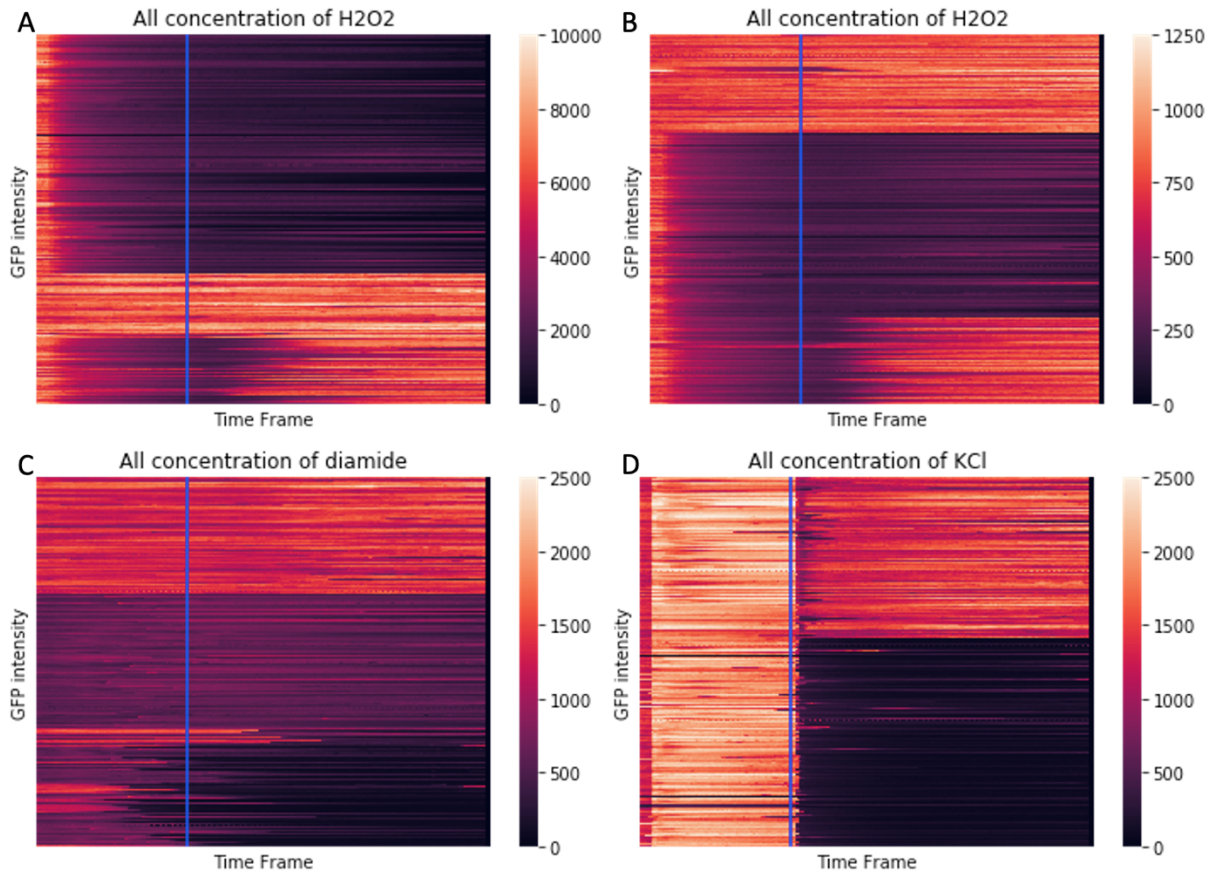
Figure 10. Heatmaps of clustering results of 2 strains under 3 types of stresses. In all panels, the x-axis stands for the time frame of the experiment from 1 to 186; the y-axis represents the intensity of GFP fluorescence within different ranges. The blue line in the plots is the x=62 line, which corresponded to the moment when the stress solution stopped entering the cells. (A) Heatmap of the clustering result of NH1284 cells under 4 concentrations of H_2O_2 solution. (B) Heatmap of the clustering result of NH1435 cells under 4 concentrations of H_2O_2 solution. (C) Heatmap of the clustering result of NH1284 cells under 4 concentrations of diamide solution. (D) Heatmap of the clustering result of NH1284 cells under 4 concentrations of KCl solution.

DISCUSSION

From the observation of GFP fluorescence recovery in some yeast cells to the analysis of the responses to different concentrations of each stress to the summary of heterogeneity of cells in response to 3 types of oxidative stresses, we combined the application of microfluidic platform, the time-lapse microscopy, and the computational data clustering methods to approach the characteristics and mechanisms of the phenotypic heterogeneity of homogenous yeast cells under different oxidative stresses. In the process, we revealed different aging patterns of yeast cells under oxidative stresses based on their stress responses, with the "no effect", "recovery", and "no recovery" types being the most representative ones in the experiment with H_2O_2 stress. We also identified one of the main factors of the mechanisms of distinct stress responses, which is the ability to regulate intracellular pH. The other two stressors provided interesting results as well, especially when we discovered that almost all cells had a higher GFP intensity during the stage of KCl stress of all concentrations (Figure 9, 10D).

Admittedly, this study is limited in many ways with the primary limiting factor being the number of trials. Although some experiment conditions were repeated, only the results from one experiment were analyzed for each strain and stress settings. Apart from the constraint on time, the consistency of data was also in consideration since the absolute value of fluorescence varied in different trials. Given these situations, it was reasonable that some plots were not explained perfectly. One representative example is the heatmaps of the clustering result of cells under the diamide stress. Despite the possibility of two-stress model, it was still confusing that the GFP intensity of many cells dropped further to a lower level after the stress was removed (Figure 7, 10C). Additionally, the application of K-Means method restricted the analysis in the range of

classification and generalization. To deduce the full mechanism from gene expression to adaptive homeostasis, quantitative approaches are indispensable.

Evidently, however, the future directions of this study might not start with quantitative analysis. Besides the number of trials, the design of the experiment process could be modified at first. For instance, it might be theoretically more efficient if we used the pHluorin in all stress conditions for a better detection of pH changes. The reason we did not was that its transfection caused all kinds of trouble. Even the successful strain, NH1435, had a generally lower level of fluorescence intensity than strains with normal GFP. Another critical improvement could be the variation in the experiment settings. The elongation of stress time and recovery time are the most promising ones. In the data analysis stage, we could try other clustering methods to approach the characteristics of stress responses from different angles. Furthermore, from biological perspectives, the distinct stress responses were not connected to the divergence of aging trajectories, as previous articles had stated that it contributed to the heterogeneity in the RLS of isogenic yeast cells [4].

Overall, a series of interesting phenomena in the phenotypic heterogeneity was observed and analyzed in this study. By constructing a basic model of the distinct stress responses of yeast cells, we provide a feasible approach to the research of phenotypic heterogeneity of homogenous cells. This process raises the possibility of modulating the mechanism and dynamics of the responses of single yeast cells to oxidative stresses in the sense of their aging phenotypes.

REFERENCE

[1] Ackermann, M (2015). A functional perspective on phenotypic heterogeneity in microorganisms. Nat Rev Microbiol 13, 497-508. doi:10.1038/nrmicro3491

[2] Radzinski, M. Fassler, R. Yogev, O. Breuer, W. Shai, N. Gutin, J. Ilyas, S. Geffen, Y. Tsytkin-Kirschenzweig, S. Nahmias, Y. Ravid, T. Friedman, N. Schuldiner, M. & Reichmann, D. (2018). Temporal profiling of redox-dependent heterogeneity in single cells. eLife 2018, 7:e37623, 1-33. doi:10.7554/eLife.37623

[3] Youlian Goulev, Sandrine Morlot, Audrey Matifas, Bo Huang, Mikael Molin, Michel B Toledano, Gilles Charvin. (2017). Nonlinear feedback drives homeostatic plasticity in H2O2 stress response. eLife 2017, 6:e23971, 1-33. doi:10.7554/eLife.23971

[4] Meng Jin, Yang Li, Richard O'Laughlin, Philip Bittihn, Lorraine Pillus, Lev S. Tsimring, Jeff Hasty, Nan Hao. (2019). Divergent Aging of Isogenic Yeast Cells Revealed through Single-Cell Phenotypic Dynamics. Cell Systems, 8, 1-12. doi:10.1016/j.cels.2019.02.002

[5] Mortimer, R., Johnston, J. (1959). Life Span of Individual Yeast Cells. Nature, 183, 1751-1752. doi:/10.1038/1831751a0

[6] Yang Li, Meng Jin, Richard O'Laughlin, Philip Bittihn, Lev S. Tsimring, Lorraine Pillus, Jeff Hasty, Nan Hao. (2017). Multigenerational silencing dynamics control cell aging. Proceedings of the National Academy of Sciences, 114 (42), 11253-11258. doi:10.1073/pnas.1703379114

[7] Yang Li, Yanfei Jiang, Julie Paxman, Richard O'Laughlin, Stephen Klepin, Yuelian Zhu, Lorraine Pillus, Lev S. Tsimring, Jeff Hasty and Nan Hao. (2020). A programmable fate decision landscape underlies single-cell aging in yeast. Science, 369 (6501), 325-329. doi:10.1126/science.aax9552

[8] Dodd, B.J.T., Kralj, J.M. (2017). Live Cell Imaging Reveals pH Oscillations in Saccharomyces cerevisiae During Metabolic Transitions. Sci Rep 7, 13922, 1-12. doi:10.1038/s41598-017-14382-0

[9] Hansen AS, Hao N, O'Shea EK. High-throughput microfluidics to control and measure signaling dynamics in single yeast cells. (2015). Nat Protoc, 10 (8), 1181-1197. doi:10.1038/nprot.2015.079